



Total Thyroidectomy

8

Rafael Humberto Pérez-Soto, Alicia Maybí Trolle-Silva,
and Miguel F. Herrera

Introduction

Thyroid resection, either lobectomy or total thyroidectomy, is the most common surgical endocrine operation [1]. Although in the last decades new surgical approaches have been described, conventional open thyroidectomy remains the gold standard for the surgical treatment of both benign and malignant disorders [2–9]. Since the refinement of this surgical procedure by the Nobel Prize awarded surgeon Theodore Kocher, advancements in surgical techniques and the development of ancillary tools such as surgical loupes, advanced energy devices, and intraoperative neuromonitoring (ioNM) systems have helped in diminishing operative time and procedure-associated complications. Although their use is not compulsory, it is recommended by the current scientific literature [10, 11–14]. In addition, the development of endocrine surgery training programs has significantly improved the outcomes of patients with thyroid-related disorders [15].

It is noteworthy to mention that in order to perform a thyroidectomy, it is important to have a deep knowledge of the neck's surgical anatomy and procedure indications. Before surgery, a complete clinical and biochemical patient assessment, as well as a joint discussion with the patient regarding the extent of the surgical procedure, potential complications, and expectations, is highly important [16].

Surgical Procedure

A 30-year-old woman presented to the endocrine surgery outpatient clinic with an incidentally diagnosed papillary thyroid microcarcinoma (mPTC). She was asymptomatic and biochemically euthyroid. She had an irrelevant familiar and past medical history. Using ultrasonography, a 1-cm lesion was observed near the posterior capsule of the left thyroid lobe. Fine-needle aspiration was performed, observing cytological findings consistent with papillary thyroid carcinoma. After a thorough discussion of the therapeutic alternatives, total thyroidectomy was elected.

The procedure is performed under general anesthesia using endotracheal tube for intraoperative nerve monitoring. The patient is placed in a supine position with a 30-degree chest elevation and slight cervical extension to enhance neck exposure. Both arms are tucked into the body (Fig. 8.1a, b). The neck is prepped, and anatomical references, such as the thyroid cartilage, sternal border, and incision site, are marked (Fig. 8.2). A 5-cm semi-collar skin incision is performed following Langer's skin tension lines (Fig. 8.3). Further in-depth dissection of the subcutaneous fat and transection of the platysma muscle is performed using monopolar cautery (Fig. 8.4). Myocutaneous (subplatysmal) flaps are created, first in the cephalad direction up to the upper edge of the thyroid cartilage (Fig. 8.5), followed by the cau-

Supplementary Information The online version contains supplementary material available at https://doi.org/10.1007/978-3-030-93673-0_8.

R. H. Pérez-Soto · M. F. Herrera (✉)
Department of Surgery, Division of Endocrine and Advanced
Laparoscopic Surgery, Instituto Nacional de Ciencias Médicas y
Nutrición, Salvador Zubirán, Tlalpan, Mexico City, Mexico

A. M. Trolle-Silva
Department of Anatomical Pathology, National Institute of
Medical Sciences and Nutrition Salvador Zubirán,
Mexico City, Mexico

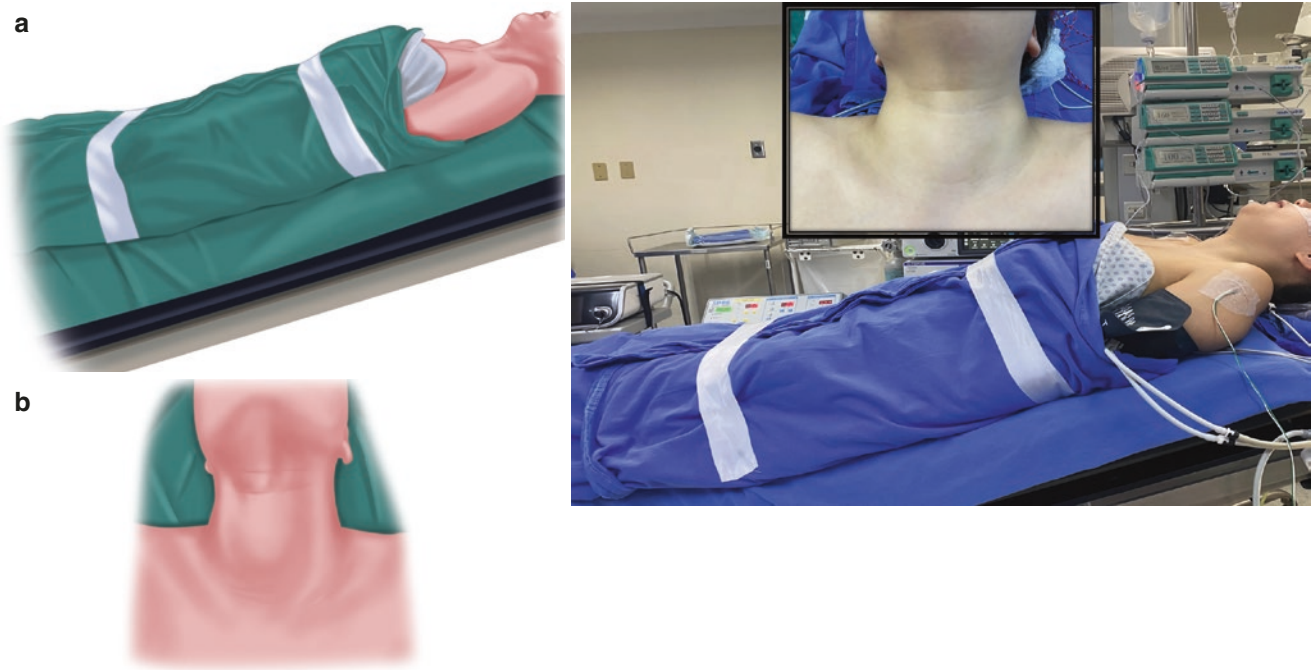


Fig. 8.1 Patient preparation. (a) Supine position with complete adduction of the arms and a 30-degree torso elevation. (b) Partial neck extension is used to improve cervical exposure

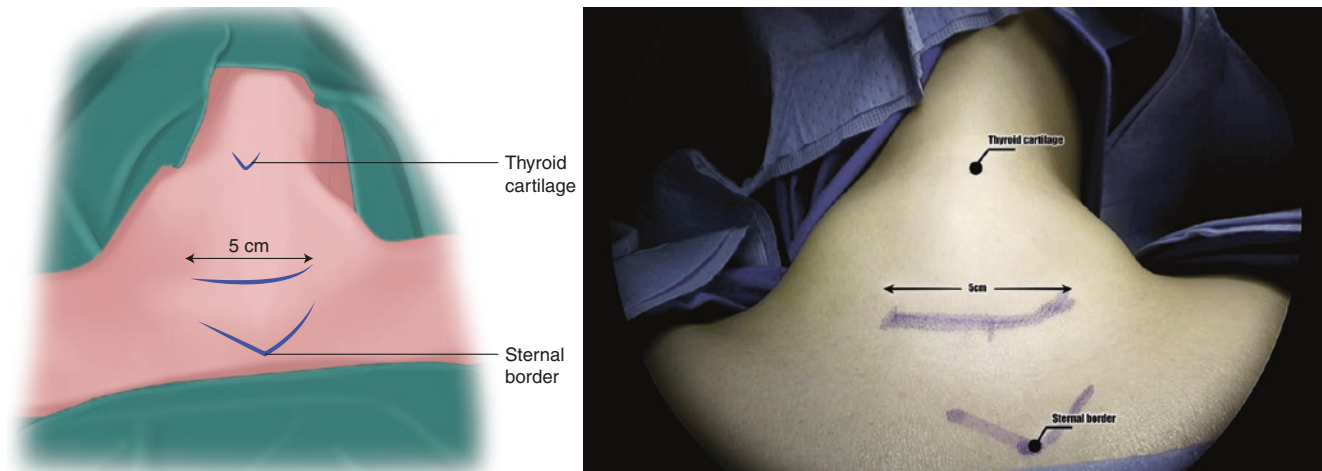


Fig. 8.2 Landmarks. Anatomical references are drawn with a surgical pen at the thyroid cartilage, superior sternal border, and incision site

dal flap up to the upper sternal border (Fig. 8.6). Special care must be taken to avoid anterior jugular vein injury. An automatic retractor is positioned. The strap muscles at the midline (*linea alba cervicalis*) are incised using ultrasonic advanced energy (Fig. 8.7).

The diseased thyroid lobe is initially approached, mobilizing the left strap muscles laterally (Fig. 8.8) until the left carotid sheath is exposed (Fig. 8.9). The left carotid sheath is

opened and the vagus nerve is identified for an initial functional evaluation (V1) using the ioNM equipment (Fig. 8.10a, b). The plane between the medial aspect of the superior pole and the cricothyroid muscle (inter-cricothyroid space) is opened (Fig. 8.11), and the external branch of the superior laryngeal nerve (EBSLN) is identified both visually and functionally (S1) (Fig. 8.12a, b). The superior vascular pedicle is controlled using ultrasonic energy, ensuring that no

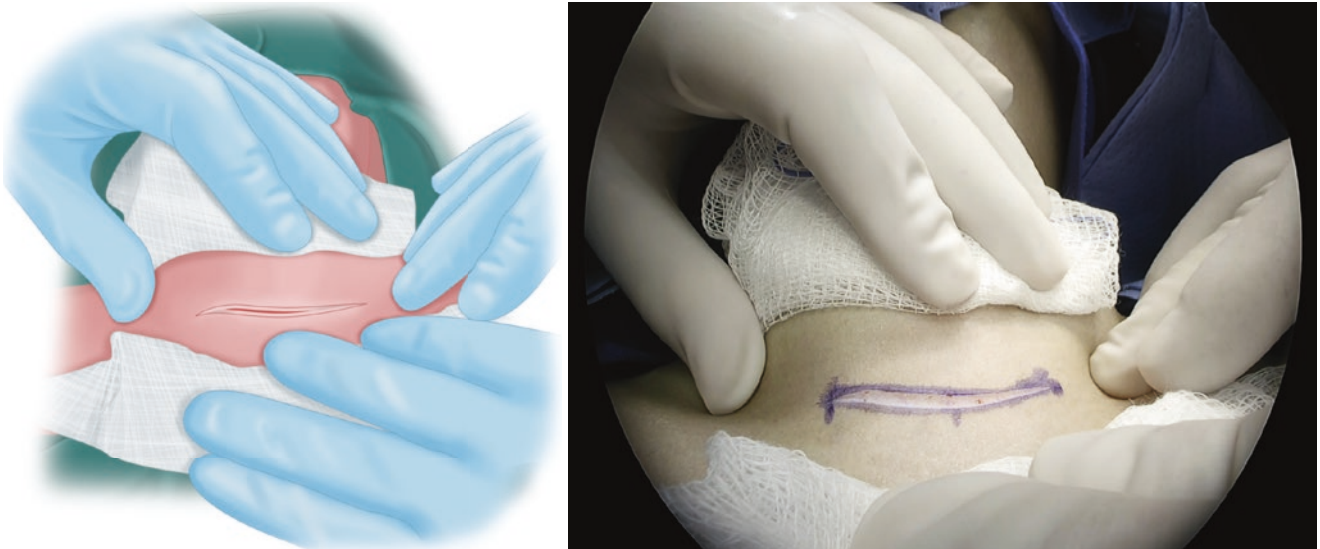


Fig. 8.3 Skin incision. A 5-cm low-collar incision following Langer's skin lines is performed using a #15 scalpel blade

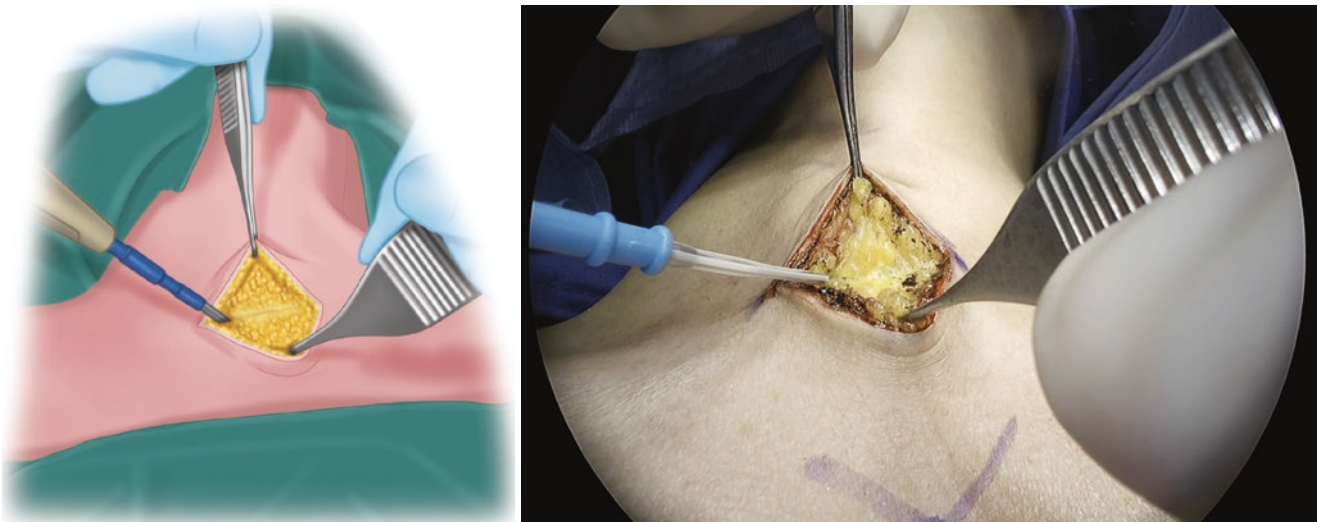


Fig. 8.4 In-depth dissection. Further in-depth dissection is carried out through subcutaneous fat tissue and platysma muscle transection using monopolar cautery

thyroid tissue is left behind and that the EBSLN is preserved (Fig. 8.13). Further lateral dissection of the upper thyroid lobe is carried out with identification and preservation of the superior parathyroid gland, along with its vascular supply (Fig. 8.14). The left recurrent laryngeal nerve (RLN) is identified visually (Fig. 8.15), and an initial functional evaluation (R1) is performed (Fig. 8.16a,b). The inferior pole of the left thyroid lobe is dissected, identifying and preserving the inferior parathyroid gland (Fig. 8.17). The branches of the infe-

rior thyroid artery are transected, the thyroid lobe is retracted medially, and Berry's ligament is divided. Lobectomy is completed with the transection of the thyroid isthmus (Figs. 8.18 and 8.19).

The left thyroid lobe is inspected, identifying the tumor (Fig. 8.20). Postdissection functional evaluation of the left vagus nerve (V2), EBSLN (S2), and RLN (R2) is performed, as well as visual confirmation of the integrity and viability of the parathyroid glands (Fig. 8.21a-d). Right lobectomy is

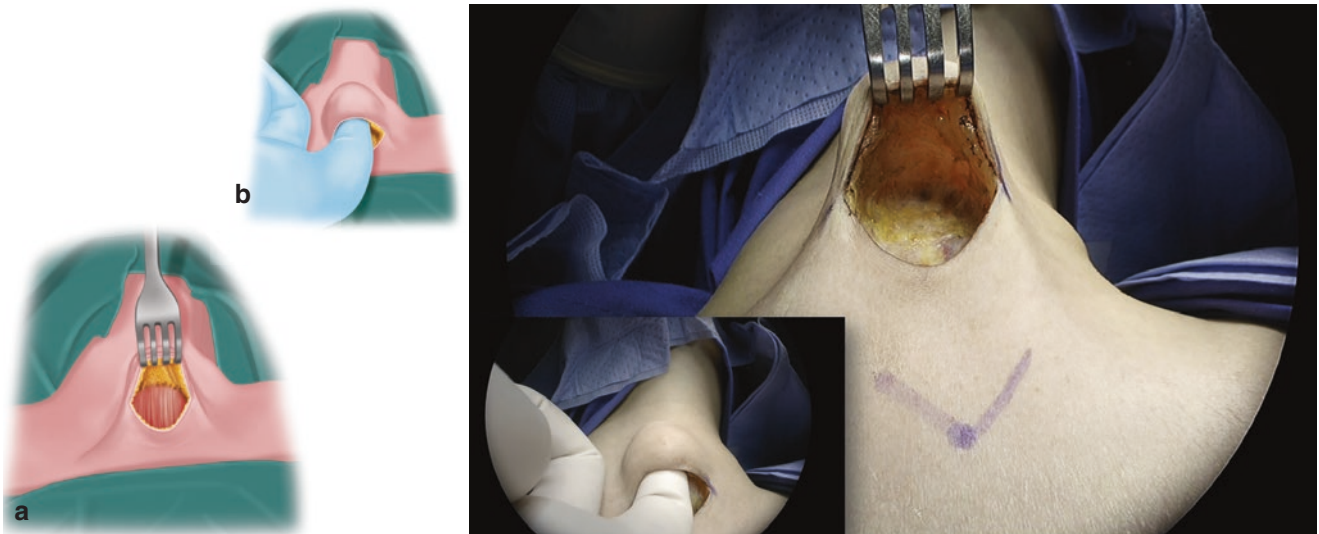


Fig. 8.5 Superior subplatysmal flap. (a) Cephalic dissection of a myocutaneous flap is performed using monopolar cautery and blunt dissection (b) until the thyroid cartilage is reached

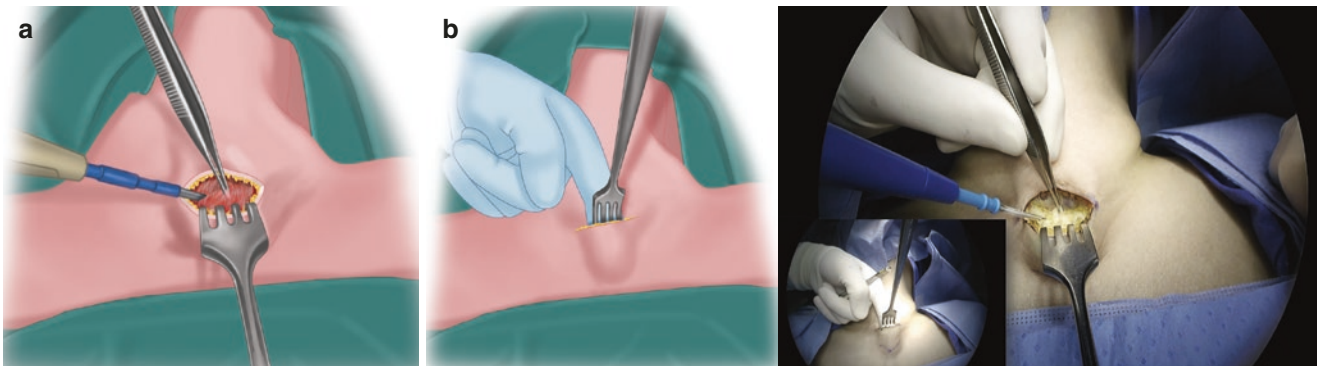


Fig. 8.6 Inferior subplatysmal flap. (a) Inferior myocutaneous flap is created (b) until the superior sternal border is identified

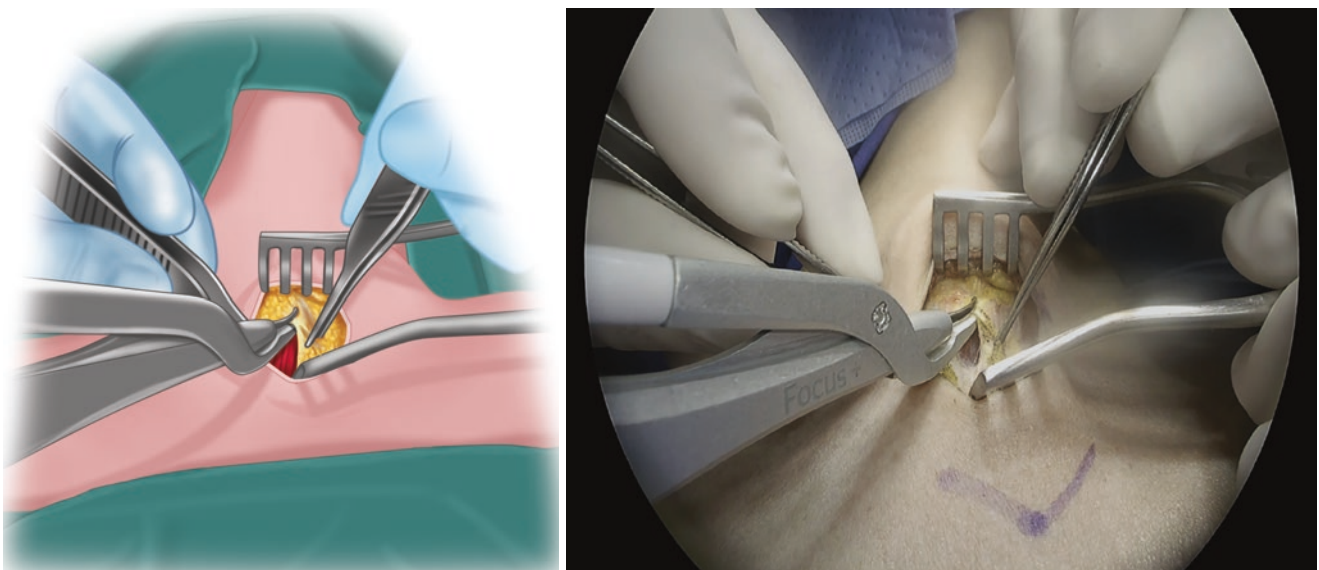


Fig. 8.7 Strap muscle midline incision. The strap muscles at the midline are identified and separated using an ultrasonic energy device

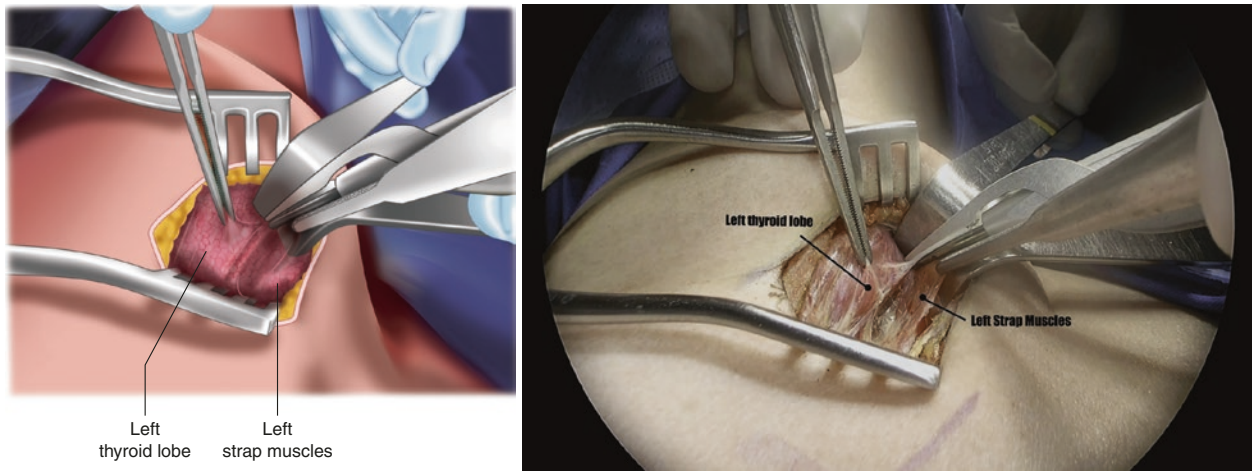


Fig. 8.8 Mobilization of strap muscles. Blunt dissection of the left strap muscles is performed to achieve their complete mobilization laterally and the exposure of the entire left thyroid lobe. Attachments of the strap muscles to the thyroid capsule are divided using an ultrasonic energy device

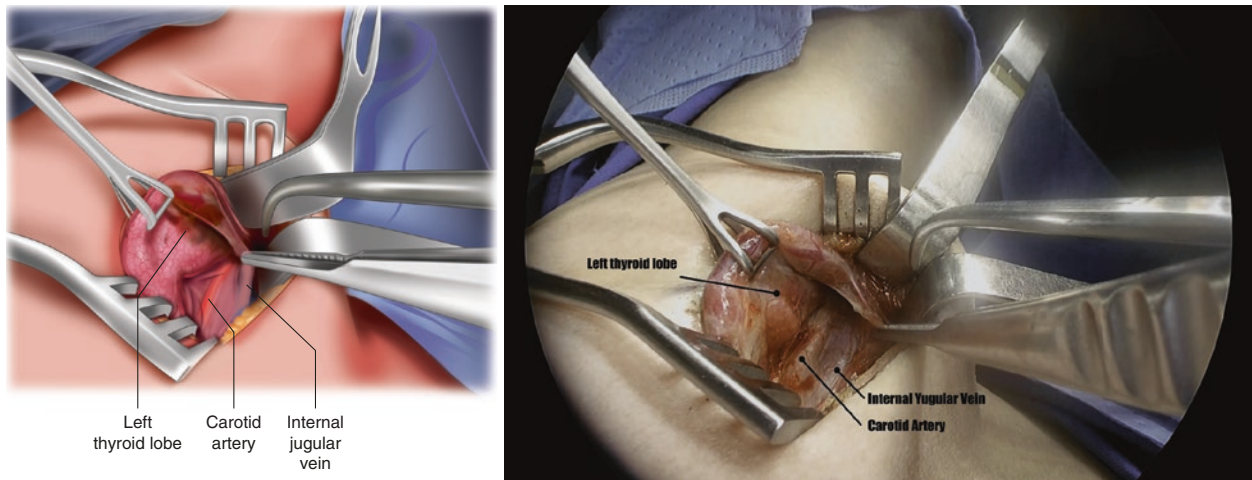


Fig. 8.9 Carotid sheath exposure. Lateral mobilization of strap muscles is continued until the carotid sheath is visualized

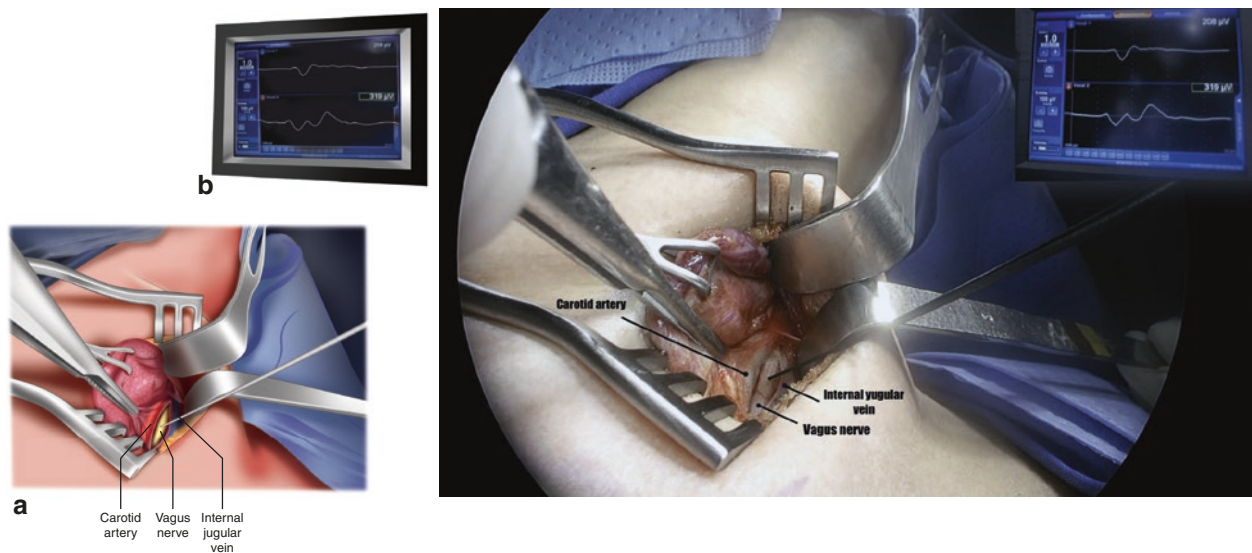


Fig. 8.10 Initial vagus nerve functional evaluation (V1). (a) The carotid sheath is opened through blunt dissection, and the vagus nerve is identified and exposed. (b) Functional evaluation is carried out with the stimulating probe of the ioNM equipment, and EMG signal is recorded in the ioNM monitor

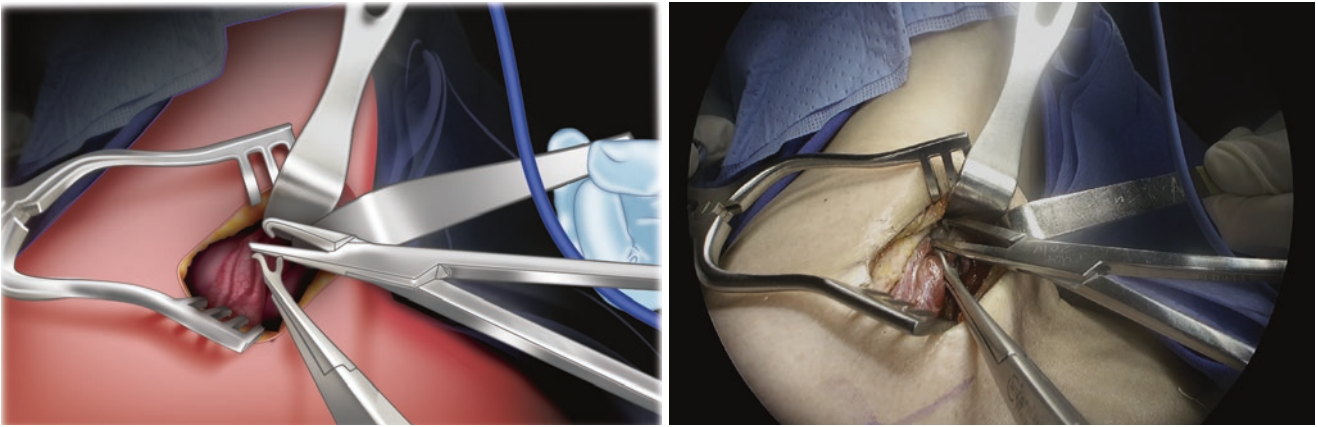


Fig. 8.11 Inter-cricothyroid space dissection. The avascular space between the upper thyroid lobe and the cricothyroid muscle is opened using blunt dissection

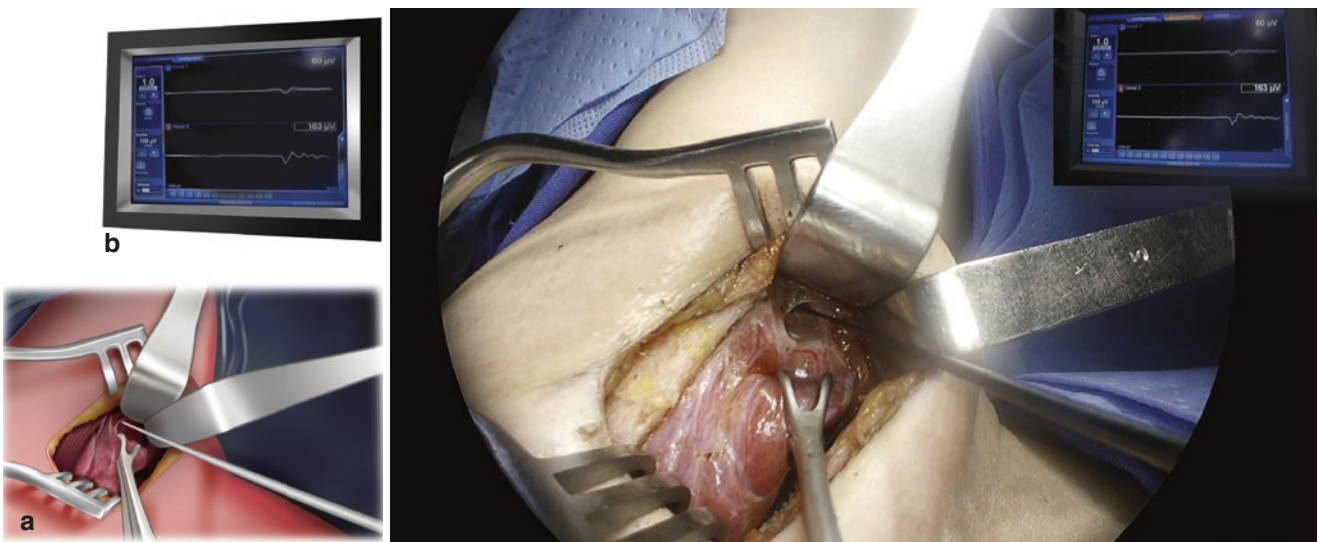


Fig. 8.12 Initial EBSLN functional evaluation (S1). (a) The EBSLN is identified within the inter-cricothyroid space, and (b) functional evaluation using the ioNM equipment is performed

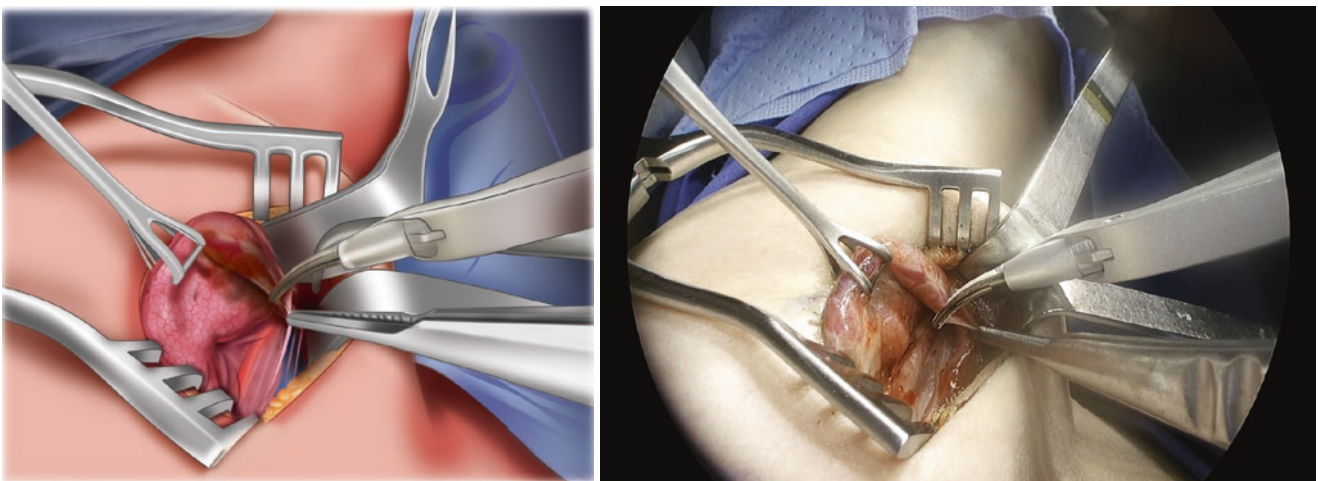


Fig. 8.13 Control of the superior vascular pedicle. Blunt dissection of the superior vascular pedicle is performed. Hemostasis and section of the superior thyroid vessels is achieved using the ultrasonic energy device

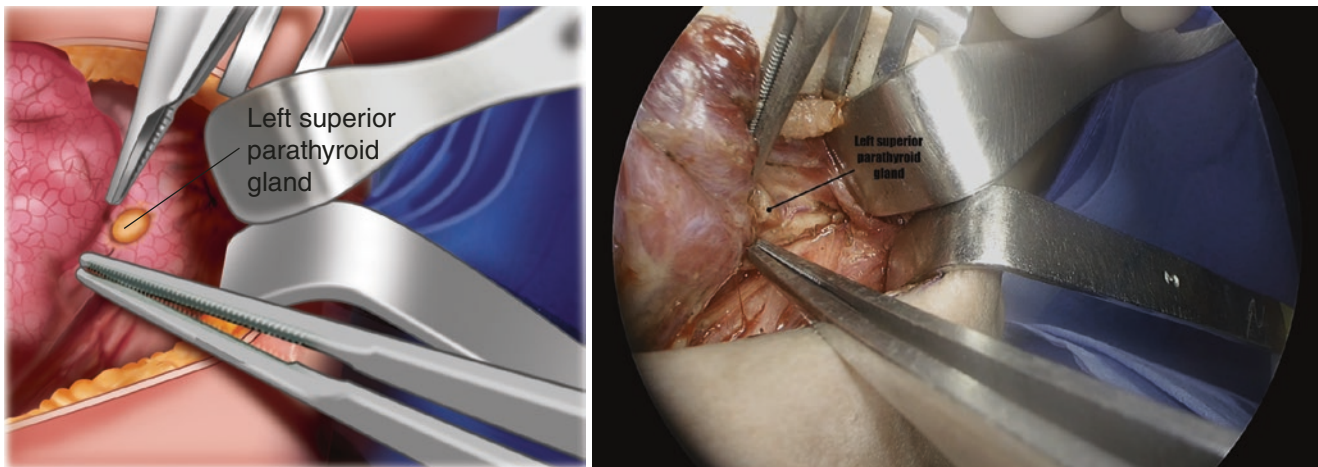


Fig. 8.14 Identification and preservation of the superior parathyroid gland. Further blunt dissection is carried out in the superior third of the thyroid lobe. Identification of the superior parathyroid gland is achieved, and careful dissection of its vascular supply is performed. The most

common anatomical reference for superior parathyroid gland localization is a 1-cm distance above the intersection of the recurrent laryngeal nerve and the inferior thyroid artery

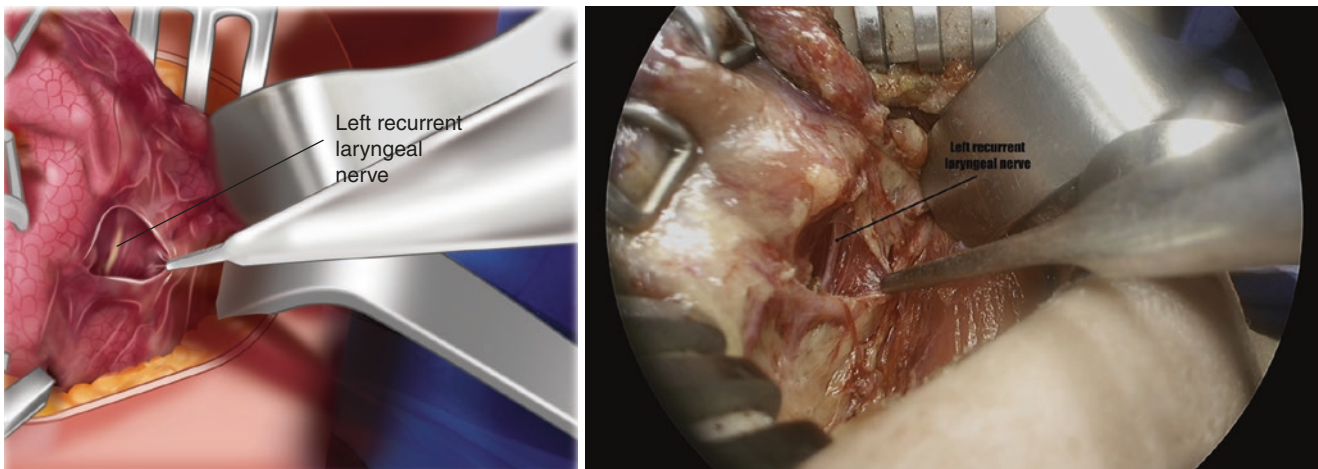


Fig. 8.15 Identification of the recurrent laryngeal nerve. Lateral blunt dissection is continued, and the RLN is identified in the tracheoesophageal groove

carried out in a similar fashion (Fig. 8.22a–f). The central neck compartment is inspected, looking for suspicious lymph nodes for metastatic disease that were absent. Hemostasis is assured, and the strap muscles are approximated using interrupted 4-0 absorbable sutures (Fig. 8.23). The platysma muscle and subcutaneous fat tissue are closed using inverted interrupted sutures with 4-0 absorbable mate-

rial (Fig. 8.24). Finally, the skin is closed with a subcutaneous running 5-0 absorbable sutures (Fig. 8.25).

Biochemical workup the day after surgery showed an albumin-corrected calcium serum level of 9.0 mg/dL (normal range: 8.6–10.3 mg/dL), phosphorus serum level of 4.6 mg/dL (normal range: 2.5–5 mg/dL), and PTH serum level of 43.10 pg/mL (normal range: 12–88 pg/mL). The patient was then discharged uneventfully (Video 8.1).

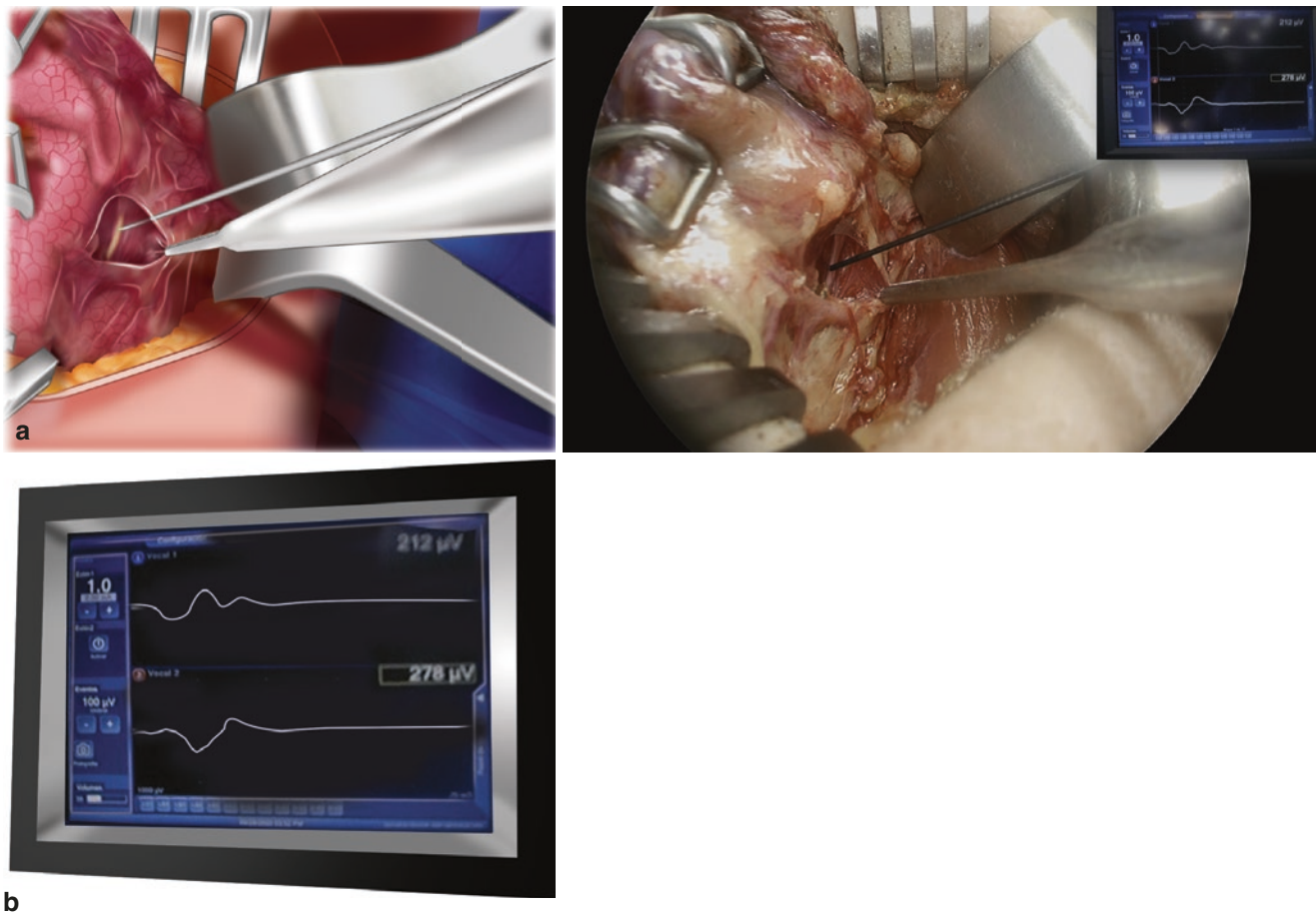


Fig. 8.16 Functional assessment of RLN. (a) The RLN is stimulated with ioNM probe, and (b) EMG signal is recorded in the ioNM equipment monitor

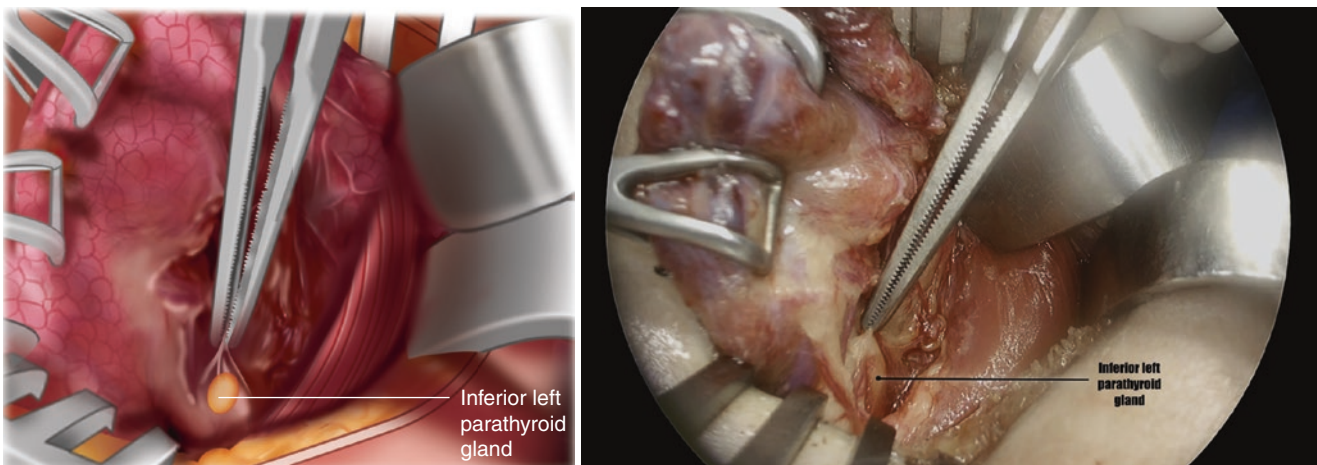


Fig. 8.17 Identification and preservation of the inferior parathyroid gland. Inferior thyroid pole is dissected, and inferior parathyroid gland identification is achieved. Subcapsular dissection prevents the injury to inferior thyroid artery branches supplying the parathyroid tissue

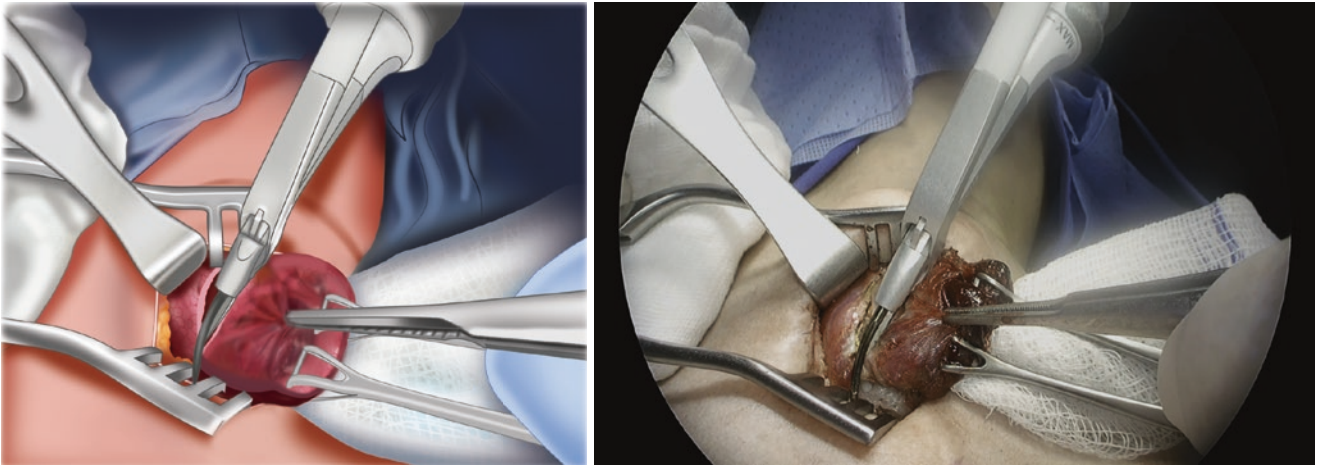


Fig. 8.18 Thyroid isthmus transection. The thyroid isthmus is transected using an ultrasonic energy device

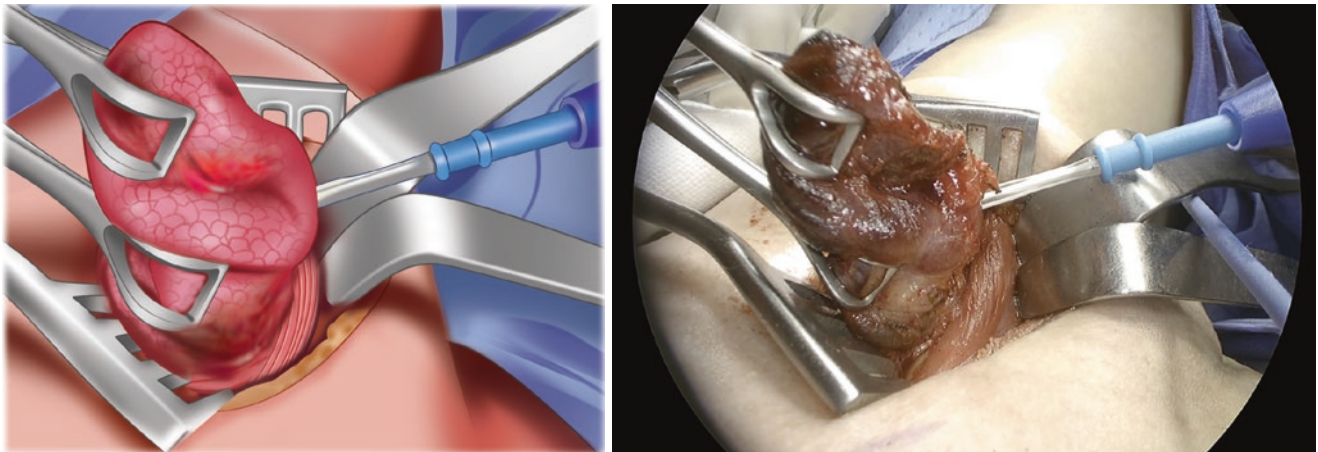


Fig. 8.19 Lobectomy. Attachments of the left thyroid lobe to the trachea are divided, assuring the safety of the RLN

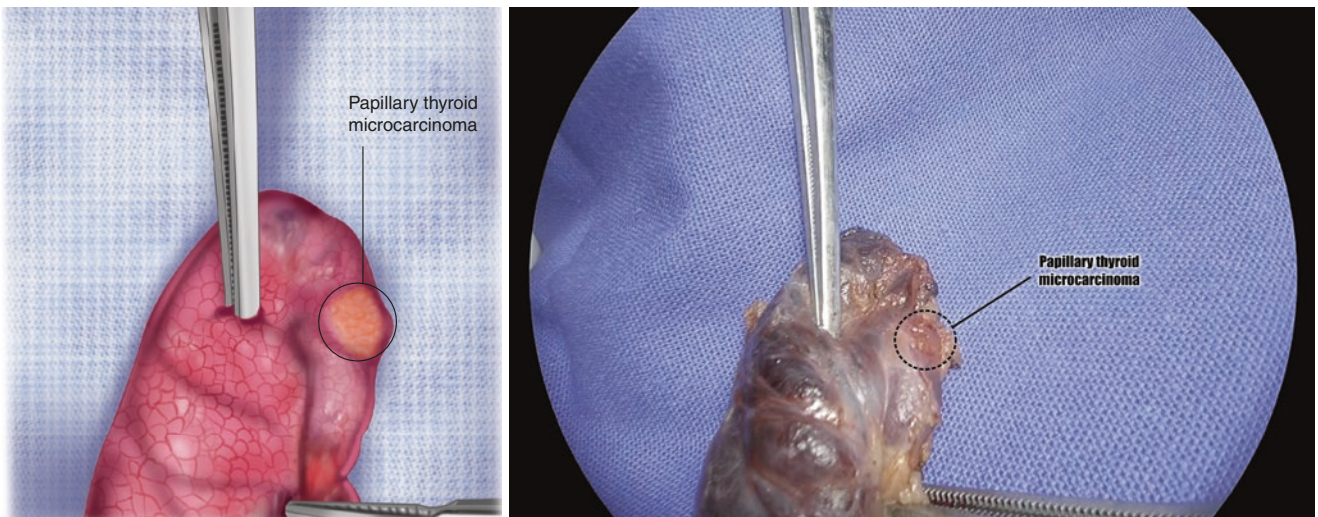


Fig. 8.20 Specimen assessment. The resected left thyroid lobe is inspected to identify the lesion and inadvertently removed parathyroid glands

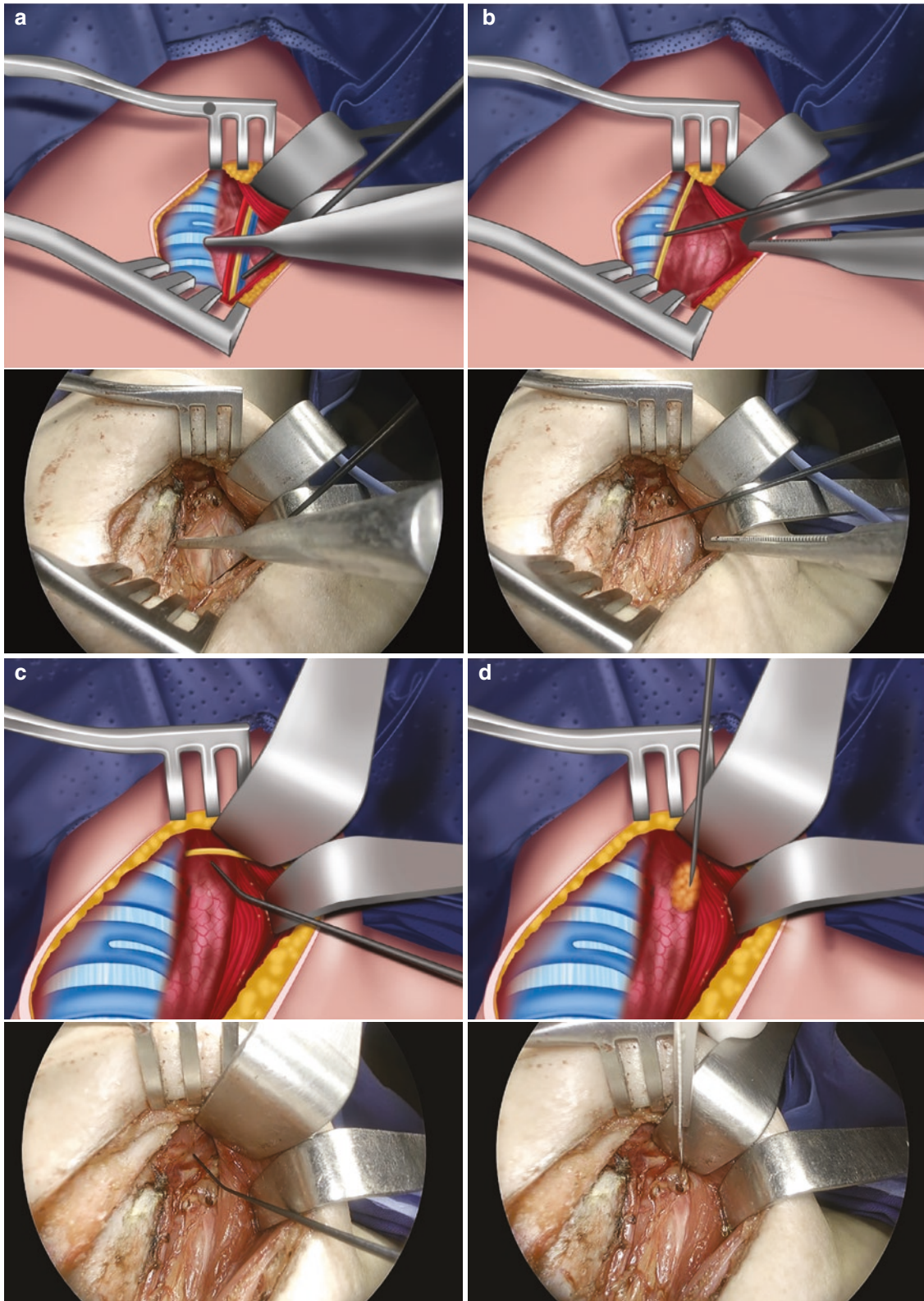


Fig. 8.21 Postlobectomy surgical field assessment. Before deciding to approach the contralateral lobe, functional evaluation of the (a) vagus nerve (V2), (b) RLN (R2), and (c) EBLSN (S2) is performed, followed by (d) parathyroid gland vascular supply assessment

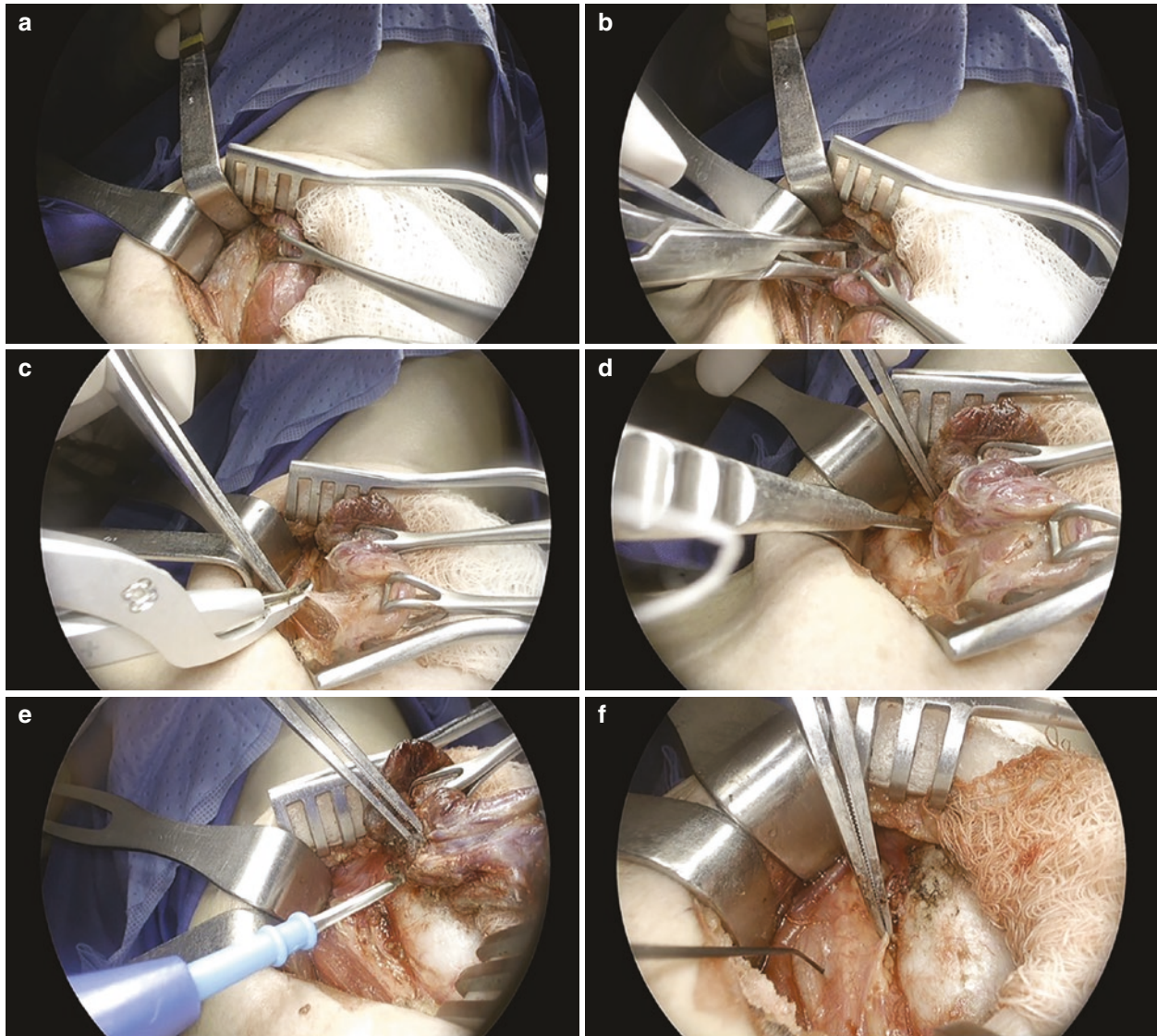


Fig. 8.22 Contralateral lobectomy. Contralateral thyroid lobe resection is carried out following the same steps. (a) Strap muscles mobilization, (b) inter-cricothyroid space dissection with EBSLN identification, (c) lateral blunt dissection of the thyroid lobe with

identification of parathyroid gland tissue, (d) RNL identification, (e) transection of thyroid lobe attachments to the trachea, and (f) post-dissection nerve functional evaluation and parathyroid gland vascular supply

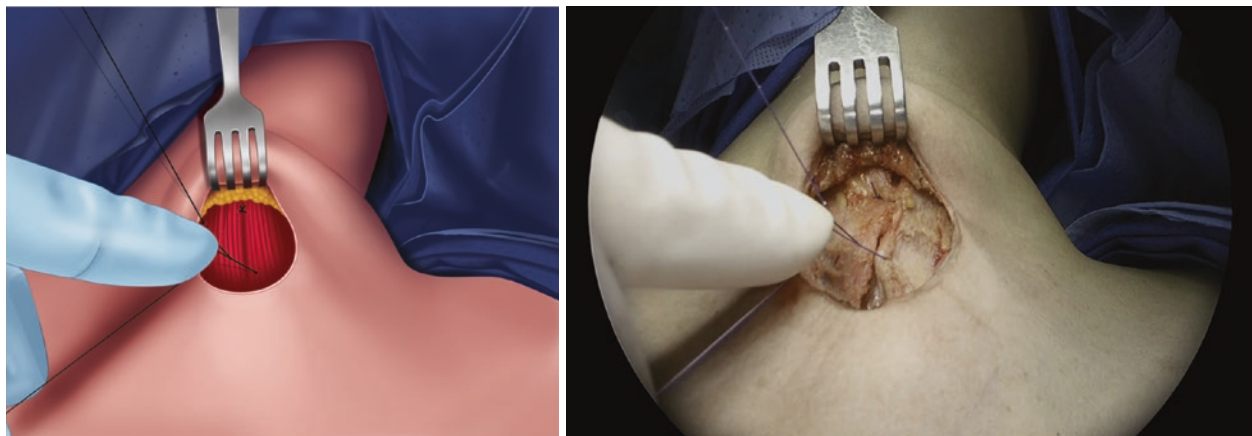


Fig. 8.23 Strap muscle approximation. The strap muscles at the midline are approximated using interrupted 4-0 absorbable sutures. Care must be taken to avoid injuries to the anterior jugular veins

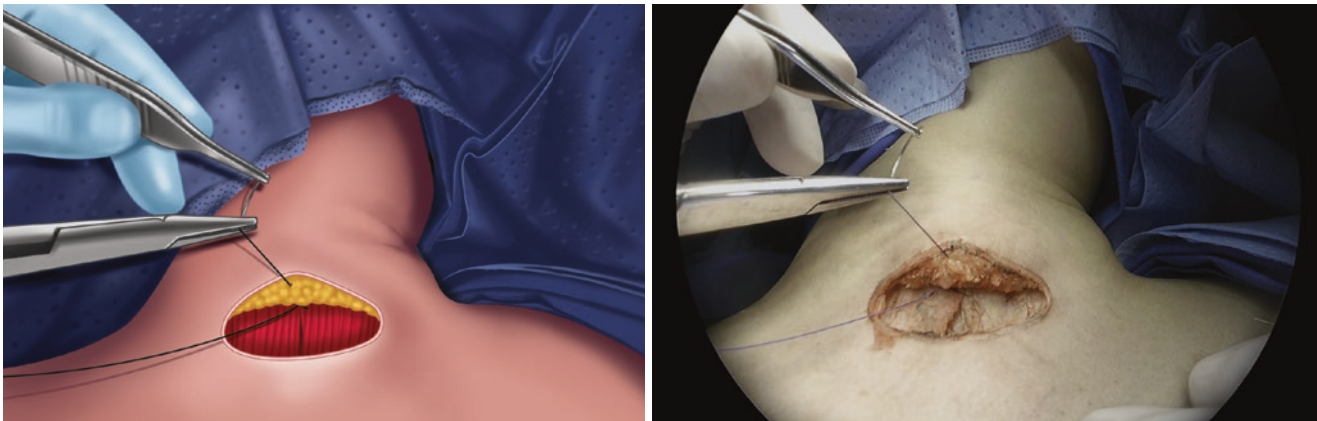


Fig. 8.24 Platysma muscle closure. The platysma and subcutaneous fat tissue are closed using inverted and interrupted 4-0 absorbable sutures

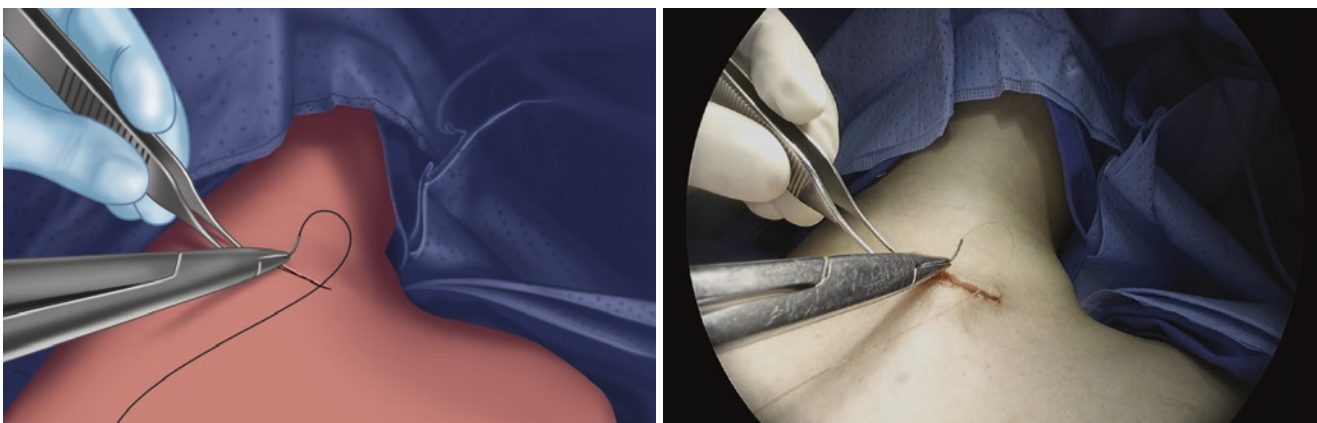


Fig. 8.25 Skin closure. A subcutaneous running 5-0 absorbable suture is used to close the skin incision

References

- Oertli D. Technique of thyroidectomy. In: Oertli D, Udelsman R, editors. *Surgery of the thyroid and parathyroid glands*. Berlin, Heidelberg: Springer; 2007. https://doi.org/10.1007/978-3-540-68043-7_7.
- Gosnell JE, Clark OH. Surgical approaches to thyroid tumors. *Endocrinol Metab Clin N Am*. 2008;37(2):437–55.
- Ikeda Y, Takami H, Sasaki Y, Kans S, Niimi M. Endoscopic neck surgery by the axillary approach. *J Am Coll Surg*. 2000;191(3):336–40.
- Ohgami M, Ishii S, Arisawa Y, Ohmori T, Noga K, Furukawa T, Kitajima M. Scarless endoscopic thyroidectomy: breast approach for better cosmesis. *Surg Laparosc Endosc Percutan Tech*. 2000;10(1):1–4.
- Miccoli P, Berti P, Raffaelli M, Conte M, Materazzi G, Galleri D. Minimally invasive video-assisted thyroidectomy. *Am J Surg*. 2001;181:567–70.
- Shimazu K, Shiba E, Tamaki Y, Takiguchi S, Taniguchi E, Ohashi S, Noguchi S. Endoscopic thyroid surgery through the axillo-bilateral-breast approach. *Surg Laparosc Endosc Percutan Tech*. 2003;13(3):196–201.
- Choe JH, Kim SW, Chung KW, Park KS, Han W, Noh DY, Oh SK, Youn YK. Endoscopic thyroidectomy using a new bilateral axillo-breast approach. *World J Surg*. 2007;31(3):601–6.
- Terris DJ, Singer MC, Seybt MW. Robotic facelift thyroidectomy: patient selection and technical considerations. *Surg Laparosc Endosc Percutan Tech*. 2011;21(4):237–42.
- Anuwong A. Transoral endoscopic thyroidectomy vestibular approach: a series of the first 60 human cases. *World J Surg*. 2016;40(3):491–7.
- Duke WS, Chaung K, Terris DJ. Contemporary surgical techniques. *Otolaryngol Clin N Am*. 2014;47(4):529–44.
- Cirocchi R, D'Ajello F, Trastulli S, Santoro A, Di Rocco G, Vendettuoli D, Rondelli F, Giannotti D, Sanguinetti A, Minelli L, Redler A, Basoli A, Avenia N. Meta-analysis of thyroidectomy with ultrasonic dissector versus conventional clamp and tie. *World J Surg Oncol*. 2010;8:112.
- D'Orazi V, Panunzi A, Di Lorenzo E, Ortensi A, Cialini M, Anichini S, Ortensi A. Use of loupes magnification and microsurgical technique in thyroid surgery: ten years' experience in a single center. *G Chir*. 2016;37(3):101–7.
- Smith RB, Coughlin A. Thyroidectomy hemostasis. *Otolaryngol Clin N Am*. 2016;49(3):727–48.
- Schneider R, Machens A, Lorenz K, Dralle H. Intraoperative nerve monitoring in thyroid surgery—shifting current paradigms. *Gland Surg*. 2020;9(Suppl 2):S120–8.
- Runkel N, Riede E, Mann B, Buhr HJ. Surgical training and vocal-cord paralysis in benign thyroid disease. *Langenbeck's Arch Surg*. 1998;383:240–2.
- Yip L, Stang MT, Carty SE. Thyroid carcinoma: the surgeon's perspective. *Radiol Clin N Am*. 2011;49(3):463–71.